Calculation of droplet deformation at intermediate Reynolds number using a Volume of Fluid technique

David S. Whyte* Malcolm R. Davidson* Steven Carnie† Murray J. Rudman‡

(Received 7 August 2000)

*Department of Chemical Engineering, The University of Melbourne, Parkville, Victoria 3052, Australia. mailto:david@vortex.chemeng.unimelb.edu.au

†Department of Mathematics and Statistics, The University of Melbourne, Parkville, Victoria 3052, Australia.

‡CSIRO - Division of Building, Construction and Engineering, Highett, Victoria 3159, Australia.

Abstract

The deformation of a droplet or bubble in simple extensional flow fields is investigated at intermediate Reynolds number using a Volume-of-Fluid (VOF) numerical algorithm (MAC2) developed by Rudman [7]. The results of an evaluation study of the MAC2 algorithm for such flows are presented. The final steady shapes of droplets in axisymmetric extensional flow fields determined by MAC2 are compared with the published numerical results of Ramaswamy and Leal [5]. This work forms the initial stage of a more comprehensive study of droplet deformation in time-dependent shear fields experienced by drops flowing through devices (e.g. homogenisers) designed for droplet breakup.

Contents

1 Introduction

Nature and industry contain many examples of liquid-liquid dispersions. Within industries such as food processing, extractive metallurgy, and in the manufacture of photographic paper, the deformation (and possible breakage) of droplets is of particular interest. The characteristic droplet size distribution of a dispersion can effect the efficiency of an industrial process. Break-up of droplets changes the mass transfer, inter-material contact and reaction surface area. Understanding droplet formation is essential in understanding how these factors can be used to change (improve) the involved process. This work forms an initial stage in the development of a full numerical model to predict droplet break-up in time-dependent shear fields within drop break-up devices used by industry e.g. homogenisers.

When the viscous and/or inertial forces of the fluid surrounding a droplet overcome the restorative force of the surface tension, droplets undergo deformation and subsequently, may break. Currently, there is no published work dealing with single droplet break-up in complex flows. So far, break-up criteria have been based on the effects of simple flow fields and order of magnitude predictions. Walstra [11], Rallison [4] and Stone [9] have reviewed droplet break-up dynamics under various conditions, none relating specifically to the types of condition expected in homogenisers.

In 1997, Ramaswamy and Leal [5] published a numerical study of deformation of droplets in steady, uniaxial elongational flow, with intermediate Reynolds number ($O(1) - O(10^2)$). The work predicts the steady-state deformed shape of droplets under flow conditions controlled by several parameters, including Reynolds and Weber numbers, density and viscosity ratios. Also, the paper reinforces the understanding of geometrical indicators of droplet failure and predicts a critical Weber number at which droplet shape becomes unstable. The present paper presents the results of a comparison study between the deformation of a droplet calculated by Ramaswamy and Leal [5], and that calculated using the Volume-of-Fluid (VOF) numerical algorithm MAC2 of Rudman [7]. The intention is to evaluate the use of MAC2 to determine steady-state droplet deformation in steady axisymmetric extensional flow and to predict the Weber number for droplet rupture.

2 Problem Statement

The velocity field and other flow characteristics to be used in the calculation are set out by Ramaswamy and Leal [5]. A Newtonian drop of constant density ($\hat{\rho}$) and viscosity ($\hat{\mu}$), is subject to a steady, axisymmetric extensional flow of a surrounding fluid also with constant density (ρ) and viscosity (μ). A uniform surface tension coefficient (γ) characterises the interface, and gravity is neglected. The far field velocity profile is given by

$$\vec{u} = \mathbf{E} \cdot \vec{r} \tag{1}$$

where

$$\mathbf{E} = E \begin{pmatrix} -1/2 & 0 & 0 \\ 0 & -1/2 & 0 \\ 0 & 0 & 1 \end{pmatrix} \tag{2}$$

and E is the principal strain rate. The density and viscosity ratios are denoted by $\lambda = \hat{\rho}/\rho$ and $\zeta = \hat{\mu}/\mu$, respectively. A schematic of a droplet in this extensional flow field is shown in Figure 1.

The problem is non-dimensionalised according to the undeformed diameter, d, as the characteristic length scale and (Ed) as the characteristic velocity. The corresponding Reynolds and Weber numbers are, respectively,

$$Re = \frac{\rho(Ed)d}{\mu}, \tag{3}$$

$$We = \frac{\rho(Ed)^2 d}{\gamma}. \tag{4}$$

These differ slightly from those in Ramaswamy and Leal [5], which were based on the undeformed radius, $\frac{1}{2}d$ as the characteristic length scale; $(\frac{1}{2}Ed)$ for the characteristic velocity.

Droplet deformation is measured using the parameter

$$D_f = \frac{(l-b)}{(l+b)}, \tag{5}$$

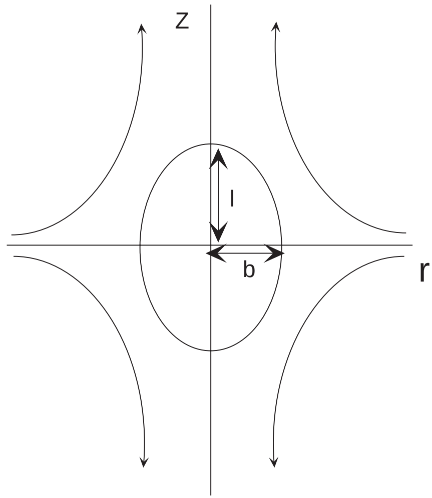

FIGURE 1: Schematic of the assumed axisymmetric extensional flow around droplet.

where l and b are the length of the major and minor axis, respectively.

3 Numerical techniques

3.1 MAC2

MAC2 is a two-dimensional, volume tracking algorithm developed specifically for solving the time-dependent, incompressible Navier-Stokes equations in fluid flows with large density variations. A piecewise linear interface reconstruction, on a grid twice as fine as that of the velocity-pressure grid, is used to maintain a sharp interface. The fractional volume function, $C(\vec{r}, t)$, used to define the 2 fluids being simulated, is advected with the local velocity on the fine grid, using the volume tracking method of Youngs [10] (also detailed in Rudman [6]). Surface tension has been included using a variant of the continuum surface force method of Brackbill *et al.* [1], described in [7]. The multigrid methods of Wesseling [12] are used to solve the pressure correction equation. The diffusion operator is explicitly applied, leading to restrictions on the time steps at low Reynolds and Weber number. The code has been applied to scenarios such as two-dimensional bubble rise in an inclined channel and a bubble bursting through an interface—this work, together with details of the implementation, is presented in Rudman [7].

The dimensionless equations of motion, ignoring gravity, solved by MAC2 are

$$\frac{\partial C}{\partial t} + \nabla \cdot (\mathbf{u}C) = 0, \tag{6}$$

$$\rho = \rho_1 C + \rho_2(1 - C), \tag{7}$$

$$\frac{\partial \rho \mathbf{u} C}{\partial t} + \nabla \cdot (\rho \mathbf{u}\mathbf{u}) = -\nabla \rho + \frac{1}{We}\mathbf{F_s} + \frac{1}{Re}\nabla \cdot \tau, \tag{8}$$

$$\nabla \cdot \mathbf{u} = 0. \tag{9}$$

Here C is the fractional volume function, advected with velocity $\mathbf{u}$, where $C = 1$ inside the droplet and $C = 0$ outside; $\mathbf{F_s}$ is the interfacial surface force.

3.2 Ramaswamy and Leal

The numerical scheme used by Ramaswamy and Leal [5] is based on that of Dandy and Leal [2], and the earlier work of Ryskin and Leal [8] and Kang and Leal [3]. This scheme is based on a finite-difference approximation of the equations of motion, applied on a boundary-fitted orthogonal curvilinear coordinate system, inside and outside the drop.

4 Numerical considerations

With the obvious symmetry in this problem, it is only necessary to solve for droplet deformation in one quadrant. In the radial direction (r) the computational domain is 1.25 drop diameters in length and is 2.5 drop diameters in the axial direction (z). Enlarging the computational domain by a factor of 2 in both directions had a negligible effect on D_f. Grid independence was checked by examining the contour lines of the fractional volume function, C. In Figure 2, contour lines of $C = 0.8$ are coincident for grids of 80×160 (80 cells in the r-direction and 160 in the z-direction) and finer. The more coarse 40×80 grid does not yield a stable D_f. There is little gained by increasing the 80×160 grid to 96×192, as shown in Figure 2; the 80×160 is therefore suitable for all calculations performed for this paper, giving 32 cells across the droplet radius. However, at higher Reynolds and/or Weber numbers, further refinement may be necessary.

The essential requirement of this study was that a clearly defined steady-state was achieved. Initially, the velocity field is taken to be zero. The field in Equation (1) is then 'turned on' gradually over 10 dimensionless time units until the desired velocity field is attained. The interface then oscillates for approximately 5 dimensionless time units before the final shape is achieved. The Figure 3, the deformed interface shape can be seen against that of the initial (or undeformed) drop shape. Determination that a steady-state has been achieved is based upon the examination of the fractional volume function contours of $C = 0.8$ and $C = 0.2$ for dimensionless times

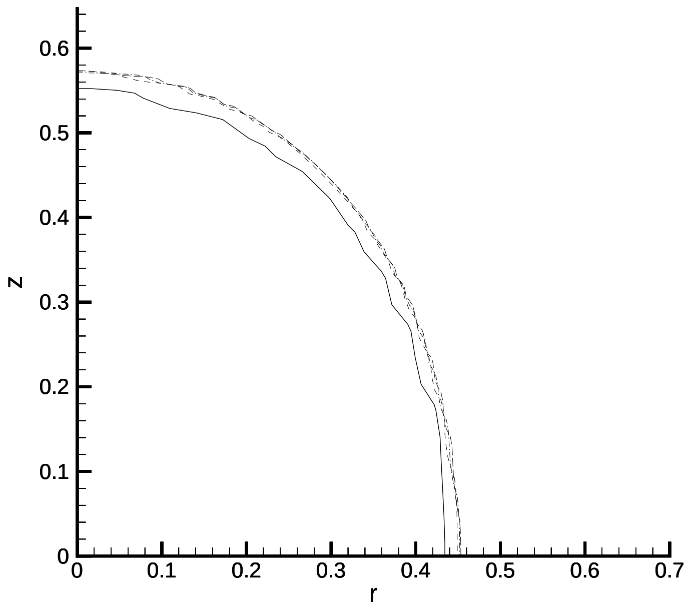

Figure 2: Grid independence: At $t = 50$, $C = 0.8$ contour lines are coincident for 80×160 (– –), 96×192 (– · –), 112×224 (· · ·) grids; also shown is the course 40×80 (—), significantly different contours.

TABLE 1: Steady-state deformation (D_f) of droplet as calculated by Ramaswamy and Leal [5] and using MAC2, for $Re = 200$, and $\lambda = \zeta = 1$.

D_f	$We = 4.0$	5.2	5.6	6.0	6.2	6.4	6.52
Ram.& Leal	0.09	0.14	0.16	0.185	0.21	0.235	0.25
MAC2 ($C = 0.8$)	0.078	0.122	0.135	0.159	0.168	0.184	0.195
MAC2 ($C = 0.2$)	0.075	0.116	0.134	0.150	0.172	0.178	0.187

$t = 25$ and $t = 50$, which are evidently coincident (see Figure 3). Hereafter, calculations on D_f will be made at $t = 25$.

5 Results and discussion

Due to computational and time limitations, only a few cases considered by Ramaswamy and Leal [5], are shown. Calculations with Re and We equivalent to the Ramaswamy and Leal values of, $\hat{Re} = \frac{1}{2}Re = 100$ and $\hat{We} = \frac{1}{4}We$ ranging from 1 to 1.63, and $\lambda = \zeta = 1$ were performed. The calculated steady-state deformation of droplets at $t = 25$ are compared in Table 1 with the corresponding values calculated by Ramaswamy and Leal [5].

It is clear from these results that the predicted deformation of droplets undergoing axisymmetric extensional flow is than that determined by Ramaswamy and Leal [5]. The discrepancy increases from 12% at $We = 4.0$

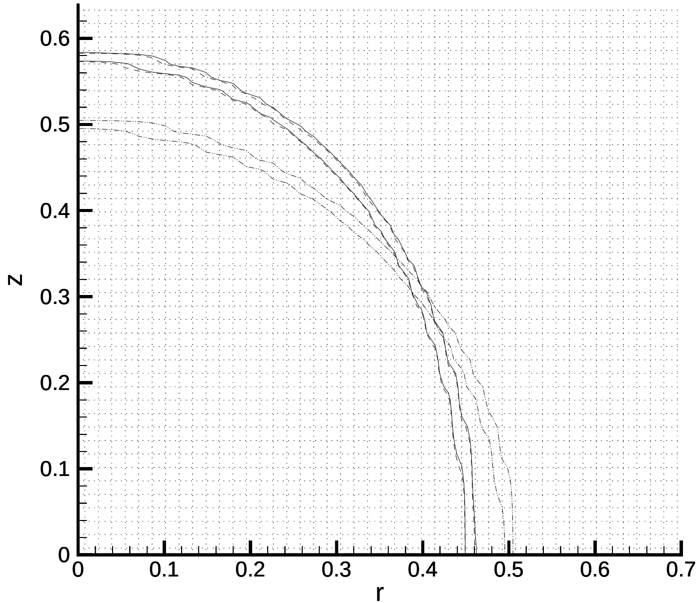

FIGURE 3: Deformation of droplet interface and steady-state: The undeformed interface is shown (– · –), and coincident interfaces for $t = 25$ (– –) and $t = 50$ (—). Inner line $C = 0.8$ contour and outer line, $C = 0.2$ contour line.

to 22% at $We = 6.52$ ($\hat{W}e = 1.63$) which is the critical Weber number (We_{crit}) for droplet rupture predicted by Ramaswamy and Leal [5]. Tests run with MAC2 determined a somewhat larger value value of $(We_{crit}) = 7.0$ with $D_f \approx 0.3$. The relatively large difference between the predictions from MAC2 and Ramaswamy and Leal [5] are in part due to the sensitivity of $D_f = (l - b)/(l + b)$ to small changes in b and l which are of similar magnitude. A new variant of the surface tension algorithm has been developed by Cummins and Rudman [Private Communication] and has been shown to be more accurate and robust. It is anticipated that implementation of this method in MAC2 will improve agreement with Ramaswamy and Leal [5].

For $We > We_{crit}$, the interface at its intersection with the r-axis becomes convex (forms a waist), and the droplet rapidly stretches until rupture occurs. The development of a convex interface appears to be the geometrical indicator of imminent droplet failure. This finding is consistent with Ramaswamy and Leal [5] and Ryskin and Leal [8]

6 Conclusion

The Volume-of-Fluid algorithm, MAC2, has been used to calculate the deformation of a droplet in axisymmetric extensional flow. The magnitude of this deformation, as measured by the ratio of the difference to the sum of the drop axes, is 10–20% less than that predicted by Ramaswamy and Leal [5]. The critical Weber number for droplet breakage, at $Re = 200$, has been determined to be 7.0, slightly higher than 6.52 predicted in [5]. Formation of a convex interface on the minor axis, as a geometrical indicator of droplet failure, is as expected.

Acknowledgements: The work was supported by the Australian Research Council in the form of an Australian Postgraduate Award (Industry) and by Kodak (Australasia) Pty Ltd.

References

[1] J.U. Brackbill, D.B. Kothe, and C.A. Zemach. A continuum method for modelling surface tension. *J. Comp. Phys.*, 100:335–354, 1992.

[2] D.S. Dandy and L.G. Leal. Buoyancy-driven motion of a deformable drop through a quiescent liquid at intermediate Reynolds number. *J. Fluid Mech.*, 208:161–192, 1987.

[3] L.S. Kang and L.G. Leal. Numerical solution of axisymmetric, unsteady free-boundary problems at finite Reynolds number. I. Finite-difference scheme and its application to the deformation of a bubble in a uniaxial straining flow. *Phys. Fluids*, 30(7):1929–1940, 1987.

[4] J.M. Rallison. The deformation of small viscous drops and bubbles in shear flows. *Ann. Rev. Fluid Mech.*, 16:45–66, 1984.

[5] S. Ramaswamy and L.G. Leal. A note on inertial effects in the deformation of Newtonian drops in a uniaxial extensional flow. *Int. J. Multiphase Flow*, 23(3):561–574, 1997.

[6] M. Rudman. Volume tracking methods for interfacial flow calculations. *Inter. J. Num. Methods*, 24:671–691, 1997.

[7] M. Rudman. A volume-tracking method for incompressible multi-fluid flows with large density variations. *Inter. J. for Num. Methods*, 28:357–378, 1997.

[8] G. Ryskin and L.G. Leal. Numerical solutions of free-boundary problems in fluid mechanics. Part 1. The finite-difference techniques. *J. Fluid Mech.*, 148:1–17, 1984.

[9] H.A. Stone. Dynamics of drop deformation and breakup in viscous fluids. *Ann. Rev. Fluid Mech.*, 26:65–102, 1994.

[10] D.L. Youngs. Time dependent multi-material flow with large fluid distortion. In K.W. Norton and M.J. Baines, editors, *Numerical Methods for Fluid Dynamics*, pages 273–285, New York, 1982, Academic Press.

[11] P. Walstra. Formation of emulsions. *Encyclopedia of Emulsion Technology - Volume 1 Basic Theory*, pages 57–128, 1983.

[12] P. Wesseling. *An Introduction to Multigrid Methods*. Wiley, New York, 1992.

C1526 C1527 C1527 C1522 C1521, C1523, C1523, C1523, C1524, C1527, C1530, C1530, C1530, C1530, C1532, C1532, C1532, C1532, C1532, C1533 C1526 C1521, C1523, C1526, C1526 C1527, C1532 C1522 C1526 C1522 C1526